

MICROWAVE OVEN SIGNAL INTERFERENCE AND MITIGATION FOR WI-FI COMMUNICATION SYSTEMS

Tanim M. Taher, Matthew J. Misurac, Joseph L. LoCicero, Donald R. Ucci
Department of Electrical and Computer Engineering
Illinois Institute of Technology
Chicago, IL 60616
Email: tahetan@iit.edu, misumat@iit.edu

ABSTRACT

The MicroWave Oven (MWO) is a commonly available appliance that does not transmit data, but still radiates signals in the unlicensed 2.4 GHz Industrial, Scientific and Medical (ISM) band. The MWO thus acts as an unintentional interferer for IEEE 802.11 Wireless Fidelity (Wi-Fi) communication signals. An analytic model of the MWO signal is developed and studied in this paper. Based on this model, an interference mitigation technique is developed that incorporates cognitive radio paradigms allowing Wi-Fi devices to reliably transmit information while a residential MWO is operating. This technique is applied in the experimental case where Barker spread Wi-Fi signals carry data in the presence of MWO emissions. Bit error rate is evaluated to provide a performance metric for the mitigation technique.

Keywords—Cognitive Radio; Wireless interference; Interference mitigation; Microwave Oven

I. INTRODUCTION

Wireless communications are the foundation of today's information-centric culture. The Federal Communications Commission (FCC) allocates many licensed bands but the Industrial, Scientific and Medical (ISM) [1] bands are unlicensed and, hence, very attractive for consumer applications. With the explosion of consumer electronics that operate in this frequency region, the 2.4 GHz ISM band has become known as the "wild west" of the electromagnetic spectrum. Devices that operate in the ISM bands, specifically the 2.4 GHz range, include all IEEE 802.11 Wi-Fi [2] access points, wireless laptops, Bluetooth devices, cordless phones, wireless video game controllers, baby monitors, and the list continues to expand.

There are also *non-data* transmitting devices operating in these bands, specifically in the 2.4 GHz range. The most common of these unintentional interferers is the MicroWave Oven (MWO). The residential MWO has one

magnetron tuned to approximately 2.45 GHz (the commercial MWO uses two magnetrons), and typically radiates across the entire Wi-Fi spectrum. This device emits electromagnetic Radio Frequency (RF) power that, when operating simultaneously and in proximity to Wi-Fi devices, can cause data loss [3] and even connection termination. For this reason, the common residential MWO is the most critical application to investigate with the goal of interference mitigation through the use of cognitive radio.

In this paper, an improved analytical model for the MWO signal is proposed, simulated, and emulated. The analytical model is key to fully understanding the interference process and this model is useful in wireless network simulation studies. The emulation provides a real-world test of the model, allowing for its verification. A cognitive radio circuit is described, which automatically mitigates RF interference from residential MWOs for a practical Wi-Fi communication system. Bit Error Rates (BERs) are measured experimentally for this system, allowing for a test of the efficacy of the interference mitigation technique. The results clearly show the feasibility and benefits of using a cognitive radio approach for mitigating MWO interference.

This paper is organized as follows. Section II examines the MWO signal characteristics. A model of the MWO signal is presented in Section III. Simulation and emulation results of the model are given in Section IV. Interference mitigation using cognitive radio is explained in Section V. Section VI describes the experimental setup used to conduct BER studies. Results of the interference mitigation, including BER tables and throughputs are presented in Section VII, followed by conclusions in Section VIII.

II. MWO SIGNAL CHARACTERISTICS

In this section, we provide an overview of the experimentally determined signal characteristics of the MWO that lead to the development of the analytical MWO model. We explore its duty cycle, frequency-sweeping phenomenon, temporal envelope, and transients.

This work is partially supported by the National Science Foundation under contract no. NSF-CNS 0520232.

The residential MWO periodically turns ON and OFF in synchronism with the 60 Hz frequency of the AC supply line powering the MWO [4]. Hence, the MWO signal is repetitive in nature with a period of 16.67 ms. Some residential models only transmit in the negative AC line cycle, while others transmit exclusively in the positive cycle. The duty cycle of all residential MWOs is thus, at most, 50%. Energy leaking from the MWO cavity causes interference in the 2.4 GHz ISM band.

The peak-power operational frequency range of the MWO varies with the manufacturer and model. For the models tested, this range was 2.45 - 2.465 GHz. The spectrogram of MWO #1 is shown in Fig. 1. Note that the shading intensity is proportional to the MWO power, i.e., the darker the image, the higher the power. This spectrogram was obtained experimentally at the Wireless Interference Laboratory (WIL), a component of the Wireless Networking and Communications Research Center (WiNCom) at Illinois Institute of Technology (IIT) using a ComBlock receiver [5]. This device mixed the MWO signal from the 2.4 GHz range down to baseband and used a 40 MHz analog to digital converter to record the MWO signal. MATLAB® software was used to obtain the spectrogram plot. The spectrogram is particularly useful in exploring the MWO emissions because it experimentally reveals the characteristics of the frequency-sweeping and transient aspects of the MWO signal.

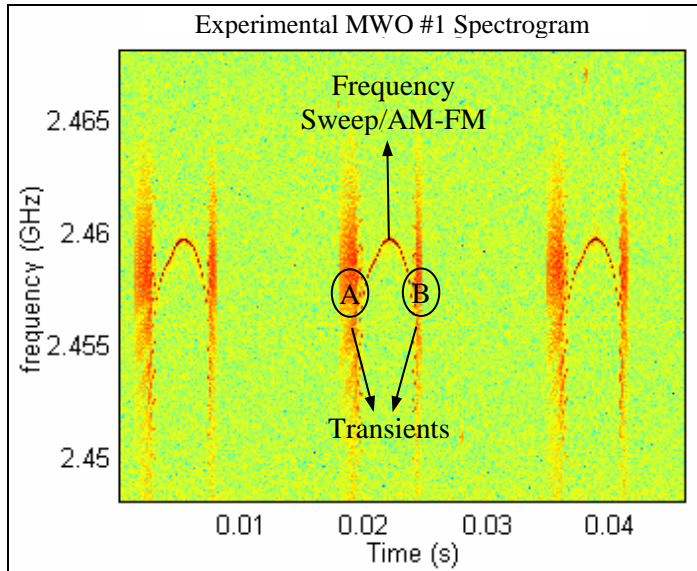


Fig. 1. Spectrogram of an actual MWO #1 signal

The residential MWO signal, in the ON mode, is similar to a Frequency Modulated (FM) signal [6] with a frequency sweep, as is clearly seen in the spectrogram in Fig. 1. The frequency-sweep in the MWO signal exists for less than half of the 60 Hz time period, typically 5-6 ms. During the frequency-sweeping part of the ON cycle, the radiated signal can be characterized as an FM signal with varying

power levels. The latter property lends itself to an Amplitude Modulated (AM) mode [6]. Thus, a combined AM-FM waveform will serve as a basis for the frequency-sweeping part of the signal [7]. The sinusoidal shape in Fig. 1 shows that the FM modulating signal can be well approximated by a sinusoid with a 60 Hz frequency.

The envelope of the MWO signal varies significantly during the ON cycle. This was observed from a detailed study of the spectrogram. Additionally, this is observed from the experimentally measured time domain envelope of the RF MWO #1 signal that is shown in Fig. 2. The amplitude of the MWO signal can be approximated by a sinusoidal waveform when the microwave oven is on.

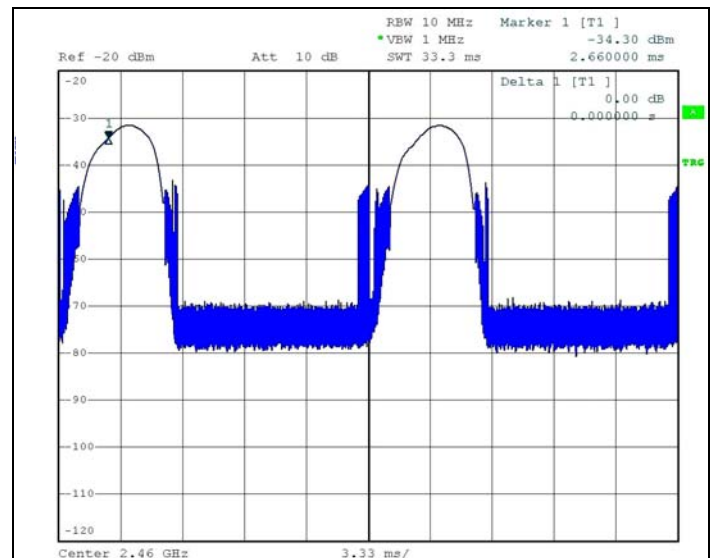


Fig. 2. The envelope of the MWO #1 signal over two 60 Hz cycles (3.33 ms/div)

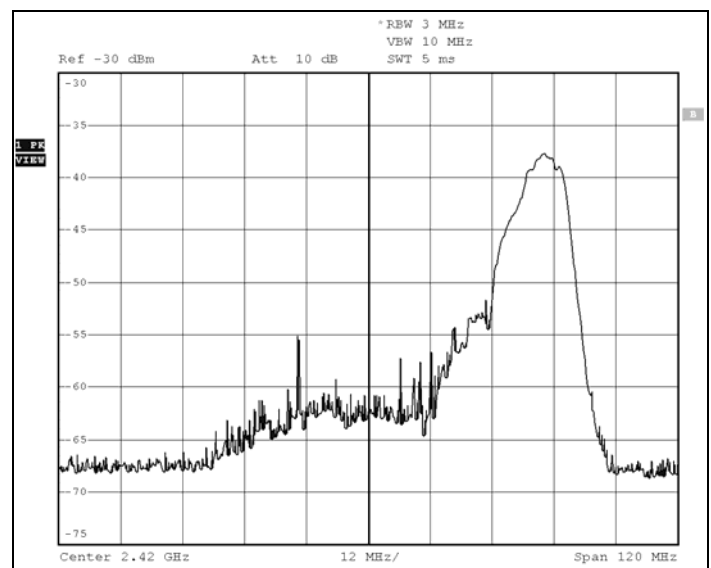


Fig. 3. Experimental PSD of MWO #1

Two transient signals, seen in Fig. 1, exist in each period; one at the beginning and one at the end of the ON cycle of

the MWO. The transient signals are broadband with Power Spectral Densities (PSDs) [6] extending up to 60 MHz in bandwidth.

The PSD of MWO #1 is shown in Fig. 3. The lower power broadband part of the PSD is caused by the transients, while the narrow band higher power part of the PSD is attributed to the frequency sweeping AM-FM signal. However, most of the power of the transients is concentrated at frequencies where the sweeping part of the MWO signal exists (see locations A and B in Fig. 1).

III. ANALYTICAL MODEL OF MWO SIGNAL

Based on the signal characteristics detailed in the previous section, an analytical model of the MWO signal was developed. The model is a derivative of an earlier model [8]. During each period, the signal can be expressed as a sum of two transients, and an AM-FM signal to represent the frequency swept signal. The modeled AM-FM signal, $s(t)$, consists of a sinusoidally modulated FM signal with a sinusoidally shaped amplitude, $x(t)$. The AM and FM modulations are both sinusoidal in nature at the 60 Hz line frequency.

The large bandwidth of the transient signals was modeled as the sum of sinc pulses modulated at different subcarrier frequencies. Figure 4 shows a qualitative plot of the time domain locations of these signals for each ON cycle.

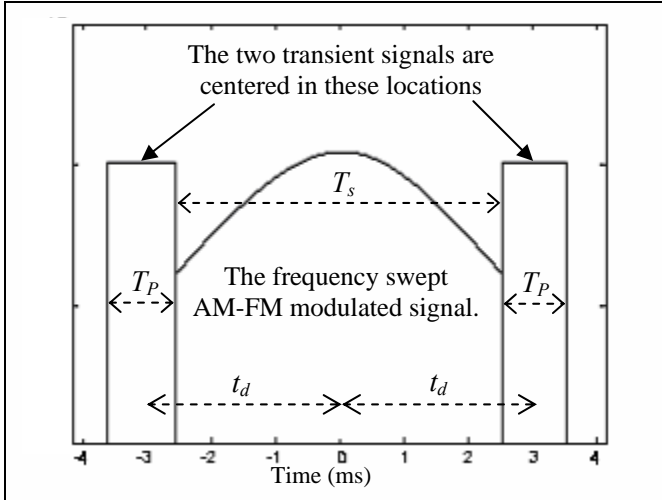


Fig. 4. Qualitative representation of MWO signal model

The complete MWO signal, $v(t)$, can be expressed as the sum of ON cycle wave-shapes, $c(t)$, that is,

$$v(t) = \sum_{n=-\infty}^{\infty} c(t - nT), \quad (1)$$

where $T = 1/f_{ac}$ and $f_{ac} = 60$ Hz.

Using the structure shown in Fig. 4 and the signal description above, the ON cycle wave-shape can be written as

$$c(t) = \sum_{n=1}^N E(f_n) p(t - t_d) \cos(2\pi f_n t) + \sum_{n=1}^N E(f_n) p(t + t_d) \cos(2\pi f_n t) + s(t), \quad (2)$$

where the transient pulse waveform is given by

$$p(t) = \text{sinc}(b(t + \lambda_n)), \quad |t| < 0.5T_p, \quad (3)$$

with b a bandwidth parameter in the kilohertz range, T_p the width of the transient pulse centered at $\pm t_d$, and λ_n a random variable uniformly distributed over $\pm 0.5T_p$ to provide a time offset for each sinc pulse in the transient signal summation.

The transient signal is the sum of N sinc pulses modulated by subcarriers, f_i , uniformly spaced from f_l to f_N . Here, f_l and f_N are the minimum and maximum values of f_i , respectively, such that $(N-1)b = f_N - f_l$. The energy in each sinc pulse is determined by the function $E(f_i)$. Several curve fitting functions were tested for $E(f_i)$ but best results were obtained with a modified Rayleigh function [6] defined as

$$E(f_i) = E_O \frac{(f_N - f_i)}{f_h^2} e^{-\frac{(f_N - f_i)^2}{2f_h^2}}, \quad (4)$$

where $f_h = f_N - f_{pk}$, (5)

E_O is an amplitude scale factor, and f_{pk} is the subcarrier frequency with the maximum transient energy.

The AM-FM signal, with sinusoidal modulation, can be written as

$$s(t) = A x(t) \cos(2\pi F_c t + \beta \sin(2\pi f_{ac} t)), \quad |t| < 0.5T_s, \quad (6)$$

where the amplitude variation is given by

$$x(t) = \cos(2\pi f_{ac} t). \quad (7)$$

The power in $s(t)$ is dictated by the amplitude, A , and the sweep time, T_s . The peak frequency deviation is determined by the modulation index, β . The carrier frequency of the AM-FM signal is a random variable F_c that is uniformly distributed between frequencies f_a and f_b . During any given period, F_c is fixed, but it varies from one ON cycle to the next.

Using the model, any MWO signal can be represented by appropriately choosing a set of 13 independent parameters. This model, when simulated and emulated, provides very good agreement to experimental measurements as detailed in the next section.

IV. MWO MODEL ACCURACY

The model described in the previous section was studied by experimentation and via simulation to examine its accuracy. An accurate model is highly useful in wireless network simulation studies. For example, simulations that study wireless network throughput and performance must account for RF interference from other radiating sources. In this case, the MWO model can be utilized as one of the wireless interferers operating in the simulated physical layer [9].

The model in Section III was simulated using MATLAB® software. Simulations were performed in the megahertz range for computational convenience. Simulations at higher and lower frequency ranges have shown that the model is scalable to all frequencies and bandwidths without altering the general signal characteristics. Figure 5 shows a spectrogram obtained using the simulated model and Fig. 6 shows the PSD. The parameters were chosen such that the PSD in Fig. 6 closely matched the characteristics of the MWO #1 PSD shown in Fig. 3. For computational feasibility, however, the MWO total bandwidth was limited in simulation to 1.5 MHz compared to the 60 MHz bandwidth of the experimental MWO #1 in Fig 3.

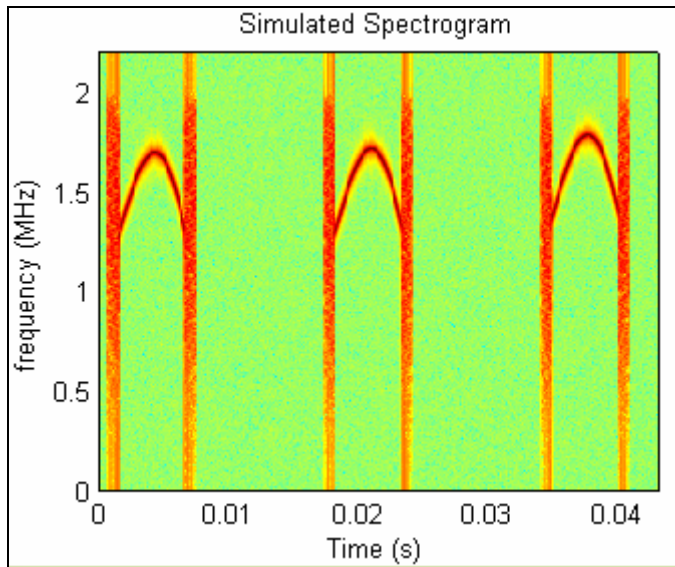


Fig. 5. Spectrogram of simulated MWO #1 signal

To verify the simulation studies and to further validate the model, the MWO model was emulated experimentally for a different MWO (#2). For this purpose, a ComBlock transmitter [5] operating in the 2.4 GHz range was used to emulate the MWO signal based on the model equations. Figure 7 shows the experimentally emulated spectrogram, and Fig. 8 is the PSD of this emulated signal obtained with a spectrum analyzer. For this emulation study, the parameters were chosen such that the PSD characteristics

closely followed that of MWO #2, the PSD of which is shown in Fig. 9. Due to experimental limitations, the emulated MWO model's bandwidth was limited to 1.5 MHz as opposed to 50 MHz for the actual MWO #2 PSD in Fig. 9.

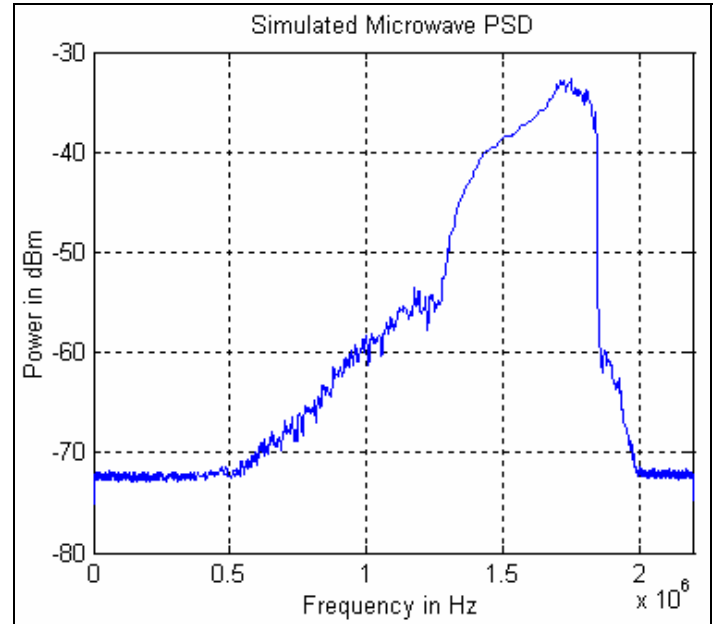


Fig. 6. Simulated PSD of MWO #1 signal

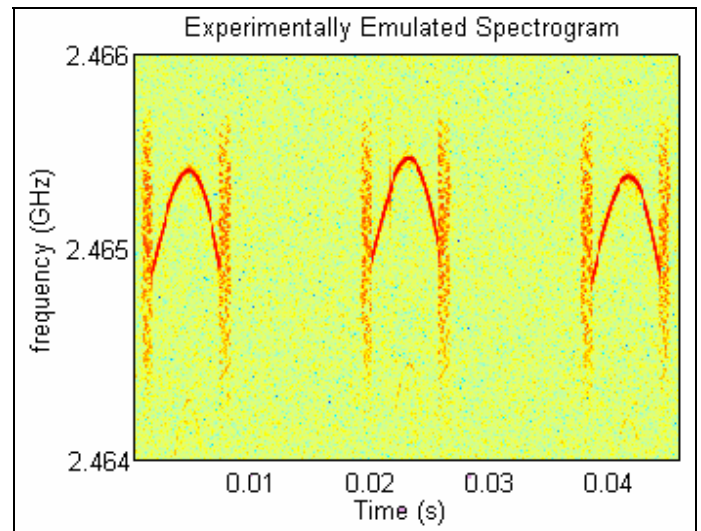


Fig. 7. Spectrogram of emulated MWO #2 signal

The simulation and emulation studies show that the model is a good approximation to the MWO signal. Furthermore, they demonstrate that the model's parameters are readily adjustable to approximately match the characteristics of different MWOs.

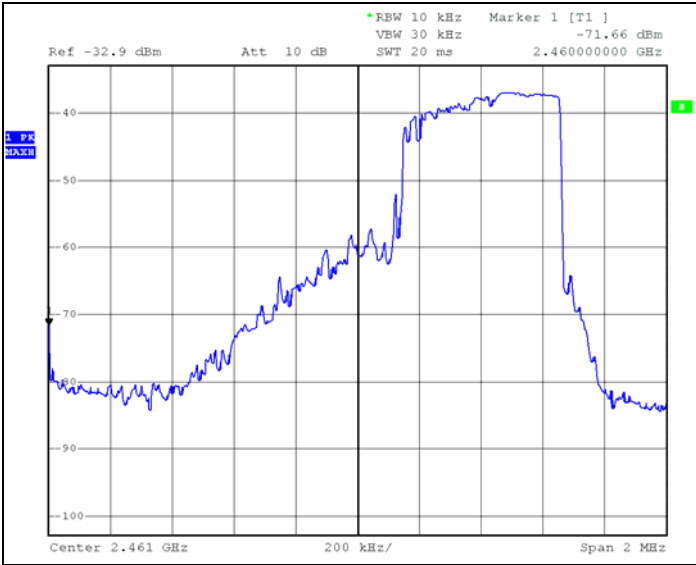


Fig. 8. PSD of Emulated MWO #2 signal measured by spectrum analyzer

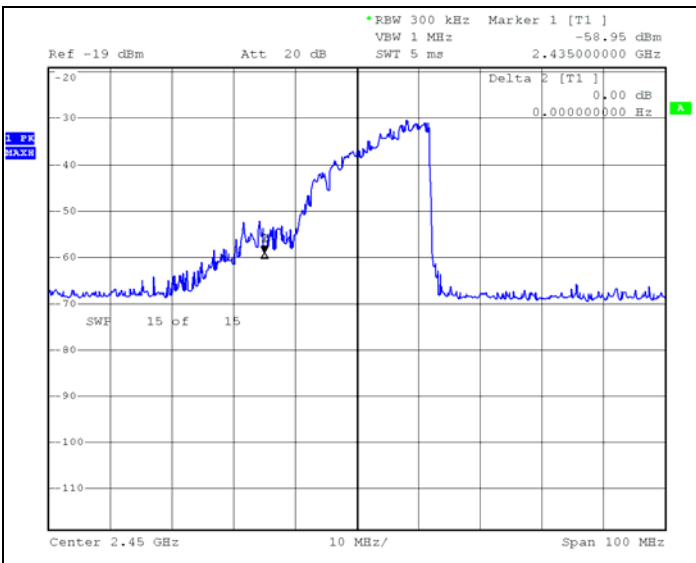


Fig. 9. Experimental PSD of actual MWO #2

V. INTERFERENCE MITIGATION TECHNIQUE

For reliable interference avoidance, Carrier Sense Multiple Access (CSMA) [10] requires that all IEEE 802.11 devices in the ISM band adhere to CSMA. However, the MWO is oblivious to the CSMA protocol. Hence, conventional interference mitigation techniques, such as CSMA, are not applicable in mitigating MWO interference.

In previous work [8], a feasible alternate interference mitigation technique was outlined. It is possible to transmit data without any MWO interference during the OFF cycles of the MWO. Figure 10 shows a qualitative plot explaining the transmission of data utilizing the interference mitigation technique presented in this paper.

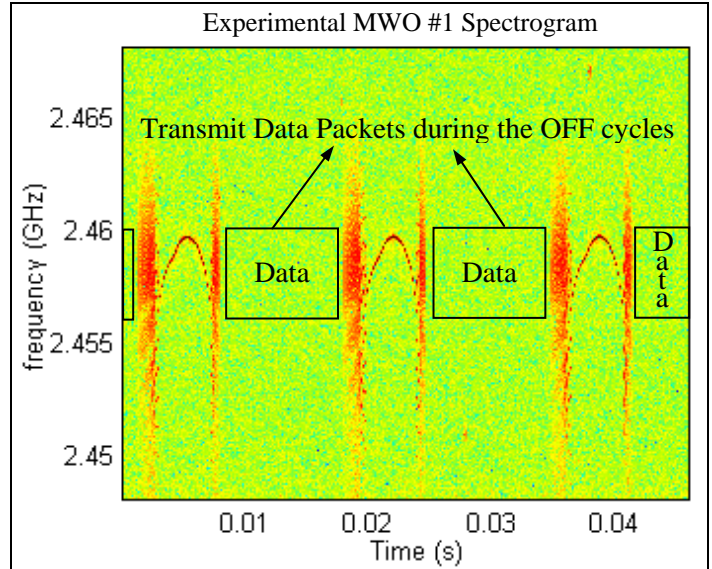


Fig. 10. Interference mitigation technique

For successful interference mitigation, it is necessary to detect the presence of MWO interference signals and synchronize the data transmitter with the MWO's ON-OFF cycles. An experimental cognitive radio system was constructed, as is shown in Fig. 11. It uses the signature of the MWO signal to detect when a MWO is operating nearby. The circuit provides a control signal that permits a Wi-Fi transceiver to communicate during the OFF cycles of the MWO, thereby mitigating the MWO interference.

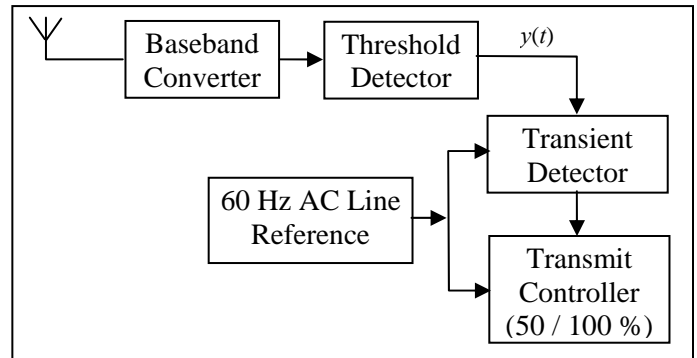


Fig. 11. Block diagram of cognitive radio system for MWO interference mitigation

The 2.4 GHz ISM band signal received by the antenna is down-converted by the *baseband converter* in Fig. 11. The *threshold detector* senses any received signal above the background noise threshold. The *transient detector* compares the threshold detector output, $y(t)$, with the *AC line reference* signal. If the timing of $y(t)$ matches with the *expected transient time location* for any MWO, then the cognitive radio records the detection of one transient. The expected transient time locations are the time durations 2 ms before and after the AC line cycle crosses the zero voltage level as it goes from a positive cycle to a negative cycle or vice versa. If the transient detector records the

presence of several transient pulses over consecutive AC line cycles, the cognitive radio circuit identifies that a MWO interference signal is present. This smart radio system cognitively ignores all Wi-Fi signals and only triggers when a MWO signal is present.

If a MWO signal is present, the *transmit controller* instructs the Wi-Fi transmitter to synchronize with the AC line cycle such that it transmits only in the OFF cycle of the MWO; that is, it transmits in the half-cycle of the line reference signal during which no transient signals are detected by the transient detector. The throughput in this case is 50%. If the MWO signal is not detected, the Wi-Fi transmitter is instructed by the transmit controller to transmit normally at 100% data rate.

VI. EXPERIMENTAL WI-FI TESTBED

An experimental Wi-Fi communication system was used to transmit and receive digital data in the presence of MWO interference. The Wi-Fi signal was transmitted by the ComBlock transmitter [5] at a rate of 363 kbps with the 11 chip Barker spreading code. This data signal's bandwidth is 8 MHz. This signal was chosen because it is very similar to the 1 Mbps data rate IEEE 802.11 signal [2] that is used to transmit the physical layer convergence protocol [11] and often data for wireless local area networks. Thus, the results of this interference mitigation study applied to the 8 MHz Wi-Fi signal are well applicable to IEEE 802.11 Wi-Fi systems in general.

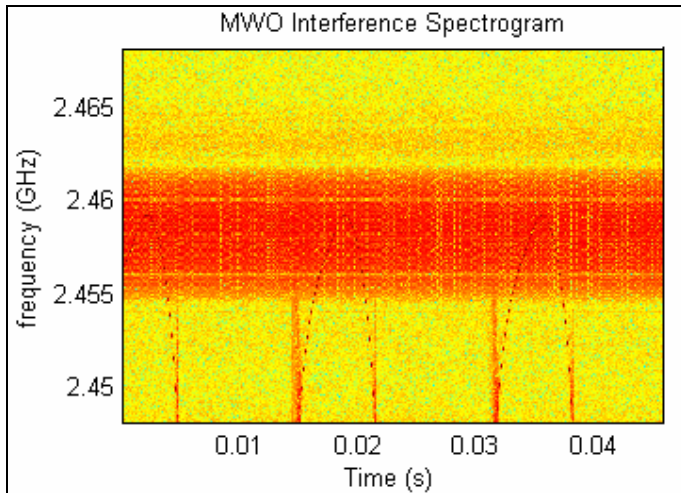


Fig. 12. Case 1: No mitigation (Wi-Fi at 2.46 GHz)

The data is transmitted in 128 bit packets by the ComBlock transmitter. The ComBlock receiver captures and decodes the data packets. The transmitted and received packets are compared to get the experimental BER. In all experiments, the receiver was placed in a position equidistant from the Wi-Fi transmitter and an interfering MWO. Three different MWOs were used in the BER study. Four experimental scenarios were tested

for each MWO and the BER was recorded each time. Case 1 is shown by the spectrogram in Fig. 12. Here the Wi-Fi transmitter operates at 2.46 GHz without any interference mitigation. In this frequency range the AM-FM signal of the MWO exists and hence there is high interference. Case 2 is shown in Fig. 13, where the interference is mitigated and the Wi-Fi transmitter frequency is still at 2.46 GHz. In Case 3 and Case 4, the Wi-Fi transmitter carrier frequency is at 2.448 GHz, where there is less interference as only low duty-cycle MWO transients exist. Interference is not mitigated in Case 3, but it is mitigated in Case 4 by the cognitive radio system.

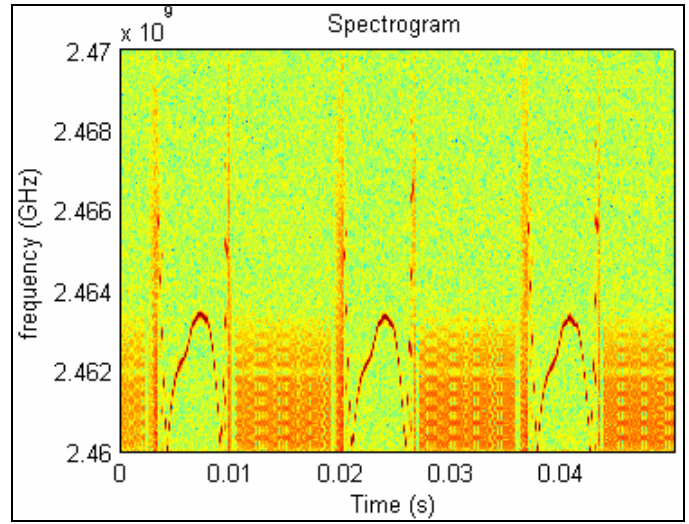


Fig. 13. Case 2: Mitigation (Wi-Fi at 2.46 GHz)

VII. INTERFERENCE MITIGATION RESULTS

Tables 1 through 4 show the experimentally recorded BERs for each of the scenarios described in Section VI. The results vary depending on the MWO used.

Table 1. BER for Case 1 (Wi-Fi at 2.46 GHz without interference mitigation)

MWO #	Data Rate	BER
1	363.3 kbps	0.016610
2	363.3 kbps	0.112900
3	363.3 kbps	0.007315

Table 2. BER for Case 2 (Wi-Fi at 2.46 GHz with interference mitigation)

MWO #	Data Rate	BER
1	181.7 kbps	0.000000
2	181.7 kbps	0.000000
3	181.7 kbps	0.000000

Table 3. BER for Case 3 (Wi-Fi at 2.448 GHz without interference mitigation)

MWO #	Data Rate	BER
1	363.3 kbps	0.002008
2	363.3 kbps	0.000165
3	363.3 kbps	0.000523

Table 4. BER for Case 4 (Wi-Fi at 2.448 GHz with interference mitigation)

MWO #	Data Rate	BER
1	181.7 kbps	0.000000
2	181.7 kbps	0.000000
3	181.7 kbps	0.000000

Although the data rate drops to 50% in the interference mitigated case, the BER is minimized. This means that data packets will be reliably transmitted by a Wi-Fi device even when a MWO is operating. In the case where this interference mitigation is not used, the data rate remains at 100% but the BER is much higher, as shown in Table 1. This means that many data packets are likely to be dropped as a result of interference and the *actual throughput* may be much less than the mitigated case even though the data transmission rate is higher. At high BER and high packet drop rates, the Wi-Fi connection may be severed [12]. The MWO interference mitigation technique solves this problem completely.

It should be noted that the Barker spread IEEE 802.11 signal is the most resistant to interference and noise effects. For other IEEE 802.11 signals the BER is likely to be higher in similar experimental settings. Also, the BER greatly depends on the relative received signal strengths of the data signal and the MWO signal, that is, the Signal-to-Interference Ratio (SIR) [13]. Due to this effect, the BER varies considerably if the distances between the receiver, transmitter, and the MWO are changed. Therefore, Tables 1 to 4 are meant only for comparative purposes to demonstrate the performance of the experimental Wi-Fi system in the different scenarios, particularly with or without interference mitigation. Tables 1 and 3 also show that MWO interference significantly degrades the wireless communication system performance making interference mitigation valuable. Furthermore, this method is practically realizable on consumer access points and other Wi-Fi devices.

VIII. CONCLUSION

The signal characteristics of the microwave oven were investigated and modeled in this paper. The model was studied experimentally and via simulation and closely matches the actual MWO signal. A cognitive radio experimental technique was implemented that successfully mitigated interference on Wi-Fi communications caused by MWO signals. This system allows Wi-Fi devices to reliably transmit data when a MWO is operating in proximity. The performance of this cognitive radio interference mitigation system was examined via BER studies and promising results were obtained.

REFERENCES

- [1] R.J. Bates, D.W. Gregory, *Voice & Data Communications Handbook (Standards & Protocols)*, 4th ed. New York, NY: McGraw Hill, 2001.
- [2] IEEE Standard 802.11: "Wireless LAN Medium Access Control (MAC) and Physical Layer Specifications," IEEE Standard for Information Technology (June 1997).
- [3] Staff, Intersil Corporation. "Effect of Microwave Oven Interference on IEEE 802.11 WLAN Reliability". IEEE P802.11-98/240. May, 1998.
- [4] A. Kamerman, N. Erkocevic, "Microwave Interference on Wireless LAN's Operating in the 2.4 GHz ISM Band," in *Proc. of IEEE PIMRC*, vol. 3, 1997, pp. 1221-1227.
- [5] Mobile Satellite Services, URL: <http://www.comblock.com/>, 2006.
- [6] J. Proakis, M. Salehi, *Communication Systems Engineering*, 2nd ed. Upper Saddle River, NJ: Prentice Hall, 1994.
- [7] Y. Zhao, B.G. Agee, J.H. Reed, "Simulation and Measurement of Microwave Oven Leakage for 802.11 WLAN Interference Management," in *Proc. IEEE International Symposium on Microwave, Antenna, Propagation and EMC Technologies for Wireless Communications*, 2005.
- [8] T.M. Taher, A.Z. Al-Banna, J.L. LoCicero, and D.R. Ucci, "Characteristics of an Unintentional Wi-Fi Interference Device – The Residential Microwave Oven," in *Proc. IEEE Military Communications Conference*, Oct. 2006.
- [9] A. S. Tanenbaum, *Computer Networks*, 3rd ed. Englewood Cliffs, NJ: Prentice-Hall, 1996.
- [10] T.S. Rappaport, *Wireless Communications Principles and Practices*, 2nd ed. Upper Saddle River, NJ: Prentice Hall, 2002.
- [11] Anatomy of IEEE 802.11b Wireless, URL: <http://www.networkcomputing.com/1115/1115ws2.html>, 2000.
- [12] Avaya Wireless Based LANs Course, URL: http://wireless.ictp.trieste.it/school_2002/lectures/ermanno/interference.ppt, 2002.
- [13] A. Goldsmith, *Wireless Communications*, New York, NY: Cambridge University Press, 2005.